


# The Combination of MR Elastography and Proton Density Fat Fraction Improves Diagnosis of Nonalcoholic Steatohepatitis

Salem Alsaqal, MD,<sup>1\*</sup>  Paul Hockings, PhD,<sup>2</sup> Håkan Ahlström, MD, PhD,<sup>1,2</sup> Anders Gummesson, MD, PhD,<sup>3</sup> Anders Hedström, MS,<sup>2</sup> Johannes Hulthe, MD, PhD,<sup>2</sup> Lars Johansson, PhD,<sup>2</sup> Heiko G. Niessen, PhD,<sup>4</sup> Corinna Schoelch, PhD,<sup>4</sup> Christian Schultheis, PhD,<sup>4</sup> Johan Vessby, MD, PhD,<sup>5</sup> Alkwin Wanders, MD, PhD,<sup>6</sup> Fredrik Rorsman, MD, PhD,<sup>5</sup> and Charlotte Ebeling Barbier, MD, PhD<sup>1</sup>

**Background:** Nonalcoholic fatty liver disease (NAFLD) is rapidly increasing worldwide. It is subdivided into nonalcoholic fatty liver (NAFL) and the more aggressive form, nonalcoholic steatohepatitis (NASH), which carries a higher risk of developing fibrosis and cirrhosis. There is currently no reliable non-invasive method for differentiating NASH from NAFL.

**Purpose:** To investigate the ability of magnetic resonance imaging (MRI)-based imaging biomarkers to diagnose NASH and moderate fibrosis as well as assess their repeatability.

**Study Type:** Prospective.

**Subjects:** Sixty-eight participants (41% women) with biopsy-proven NAFLD (53 NASH and 15 NAFL). Thirty participants underwent a second MRI in order to assess repeatability.

**Field Strength/Sequence:** 3.0 T; MR elastography (MRE) (a spin-echo echo-planar imaging [SE-EPI] sequence with motion-encoding gradients), MR proton density fat fraction (PDFF) and R2\* mapping (a multi-echo three-dimensional gradient-echo sequence), T1 mapping (a single-point saturation-recovery technique), and diffusion-weighted imaging (SE-EPI sequence).

**Assessment:** Quantitative MRI measurements were obtained and assessed alone and in combination with biochemical markers (cytokeratin-18 [CK18] M30, alanine transaminase [ALT], and aspartate transaminase [AST]) using logistic regression models. Models that could differentiate between NASH and NAFL and between moderate to advanced fibrosis (F2–4) and no or mild fibrosis (F0–1), based on the histopathological results, were identified.

**Statistical Tests:** Independent samples *t*-test, Pearson's chi-squared test, area under the receiver operating characteristic curve (AUROC), Spearman's correlation, intra-individual coefficient of variation, and intraclass correlation coefficient (ICC). Statistical significance was set at  $P < 0.05$ .

**Results:** There was a significant difference between the NASH and NAFL groups with liver stiffness assessed with MRE, CK18 M30, and ALT, with an AUROC of 0.74, 0.76, and 0.70, respectively. Both MRE and PDFF contributed significantly to a bivariate model for diagnosing NASH (AUROC = 0.84). MRE could significantly differentiate between F2–4 and F0–1

View this article online at [wileyonlinelibrary.com](http://wileyonlinelibrary.com). DOI: 10.1002/jmri.28040

Received Sep 23, 2021, Accepted for publication Dec 14, 2021.

\*Salem Alsaqal, M.D. Department of Surgical Sciences, Section of Radiology Akademiska sjukhuset 751 85 Uppsala, Sweden.

E-mail: [salem.alsaqal@radiol.uu.se](mailto:salem.alsaqal@radiol.uu.se)

Salem Alsaqal and Paul Hockings contributed equally to this work.

Fredrik Rorsman and Charlotte Ebeling Barbier contributed equally to this work.

From the <sup>1</sup>Department of Surgical Sciences, Section of Radiology, Uppsala University, Uppsala, Sweden; <sup>2</sup>Antaros Medical, Mölndal, Sweden; <sup>3</sup>Department of Clinical Genetics and Genomics, Region Västra Götaland, Sahlgrenska University Hospital, Gothenburg, Sweden; <sup>4</sup>Department of Translational Medicine and Clinical Pharmacology, Boehringer Ingelheim Pharma GmbH & Co. KG, Biberach, Germany; <sup>5</sup>Department of Medical Sciences, Section of Gastroenterology and Hepatology, Uppsala University, Uppsala, Sweden; and <sup>6</sup>Department of Clinical Medicine, Aalborg University and Aalborg University Hospital, Aalborg, Denmark

Additional supporting information may be found in the online version of this article

This is an open access article under the terms of the Creative Commons Attribution License, which permits use, distribution and reproduction in any medium, provided the original work is properly cited.

(AUROC = 0.74). A model combining MRE with AST improved the diagnosis of F2–4 (AUROC = 0.83). The ICC for repeatability was 0.94 and 0.99 for MRE and PDFF, respectively.

**Data Conclusion:** MRE can potentially diagnose NASH and differentiate between fibrosis stages. Combining MRE with PDFF improves the diagnosis of NASH.

**Level of Evidence:** 2

**Technical Efficacy:** Stage 2

J. MAGN. RESON. IMAGING 2021.

**N**onalcoholic fatty liver disease (NAFLD) is the most rapidly growing cause of chronic liver disease worldwide, affecting about 25% of the global adult population.<sup>1</sup> NAFLD is a disease spectrum whose mild form, nonalcoholic fatty liver (NAFL), is defined as the presence of hepatic steatosis without any secondary cause of hepatic fat accumulation such as excessive alcohol consumption, long-term use of a steatogenic medication, or other liver disease etiologies.<sup>2</sup> NAFLD is associated with metabolic syndrome, obesity, diabetes mellitus, dyslipidemia, and cardiovascular disease.<sup>3,4</sup> Nonalcoholic steatohepatitis (NASH) is a more aggressive form of NAFLD, characterized by the presence of inflammatory features and degenerative hepatocellular changes in addition to steatosis.<sup>5,6</sup> The overall prevalence of NASH in the general population is estimated between 1.5% and 6.45%.<sup>1</sup>

The dynamic nature of NAFLD has been described in many studies.<sup>7,8</sup> Patients with NAFLD, especially with uncontrolled metabolic disease and diabetes, suffer an increased risk of developing fibrosis with eventual progression to cirrhosis and end-stage liver disease. The presence of inflammation in NASH triggers fibrogenesis and causes progression into higher stages of fibrosis and cirrhosis.<sup>9,10</sup> NASH is also related to increased incidence of hepatocellular carcinoma<sup>11,12</sup> and liver transplantation.<sup>13</sup> Higher stages of fibrosis are associated with increased overall and liver-related mortality.<sup>14,15</sup>

Liver biopsy has been the reference standard for diagnosing NAFLD, including identifying NASH and staging fibrosis.<sup>2</sup> However, biopsy has several limitations such as cost, sampling and inter-observer variability, and risk of discomfort and complications.<sup>16,17</sup> Thus, developing non-invasive imaging and biochemical markers for diagnosing and grading NAFLD has been the subject of extensive research in the last decade.<sup>18,19</sup>

MRI techniques for the quantification of liver fat and the measurement of liver stiffness are widely studied.<sup>18,19</sup> Magnetic resonance proton density fat fraction (MR-PDFF) and magnetic resonance elastography (MRE) have high diagnostic accuracy for detecting and grading steatosis<sup>20</sup> and staging fibrosis,<sup>21,22</sup> respectively. Both techniques have higher diagnostic performance than non-MRI-based techniques, such as transient elastography (TE) and TE-based controlled attenuation parameter.<sup>22–26</sup> However, differentiating NASH from NAFL is still challenging.

The primary aim of this study was to investigate the ability of multiple MRI biomarkers (MRE, PDFF, R2\* mapping, T1 mapping, and diffusion-weighted imaging [DWI]), either as single measures or in combination with each other or with biochemical markers, to differentiate between NASH and NAFL, and between lower and higher stages of liver fibrosis in adults with clinically suspected NAFLD. The reliability of a biomarker is not only determined by its diagnostic performance, but also by its repeatability. Hence, a secondary aim was to measure the repeatability of the MRI biomarkers.

## Materials and Methods

### Study Population

After approval from the regional ethical review board, a prospective study was conducted at our hospital between March 2017 and December 2019. Written informed consent was obtained from all study participants. One hundred and thirty-four individuals, recruited from the Department of Gastroenterology and Hepatology and from the Swedish CArdioPulmonary BioImage Study “SCAPIS”,<sup>27</sup> were invited to a screening visit, where data on demographics, medical history, and concomitant medication were collected. Blood sampling was also performed at screening visit to measure cytokeratin-18 (CK18) M30 and liver function tests including alanine transaminase (ALT) and aspartate transaminase (AST).

Eligibility included: individuals aged 18–70 with clinically suspected NAFLD and at least one of the following: imaging indicative of NAFLD,<sup>19</sup> ALT more than  $1.5 \times$  upper limit of normal (upper limit being 1.1  $\mu$ kat/liter for men and 0.75  $\mu$ kat/liter for women), CK18 M30 more than 180 U/liter, and/or biopsy showing NAFLD within 3 months prior to screening visit. Individuals with a past or present alcohol consumption of more than 30 g alcohol per day for men and 20 g for women, drug abuse, other liver diseases, corticosteroid or immunosuppressive therapy within 10 weeks, pregnancy/breastfeeding, and/or contraindication for MRI or liver biopsy were excluded. Seventy-five individuals fulfilled the inclusion and exclusion criteria.

Individuals with no available liver biopsy within 3 months underwent liver biopsy 1–4 weeks after the screening visit. Three out of the 75 persons were excluded since the liver biopsy did not show any steatosis. One of the included persons discontinued the study voluntarily before MRI examination. Thus, 71 individuals were referred to MRI. Of these, three were excluded because of claustrophobia. Consequently, the study population consisted of 68 participants.

Thirty participants out of the study population (11 NAFL and 19 NASH determined from liver biopsy) underwent a second MRI in order to assess repeatability. Those participants were selected to represent various histopathological groups, i.e., including participants with both NAFL and NASH and with different stages of fibrosis.

### Histopathological Analysis

Biopsies were evaluated by two liver pathologists (AW) with more than 30 years of experience blinded to clinical, biochemical, and radiological data individually and in consensus. The steatosis-activity-fibrosis (SAF) histological scoring system was used,<sup>5</sup> grading steatosis 0–3, activity 0–4, and fibrosis 0–4. Activity score was calculated by the summation of hepatocyte ballooning (0–2) and lobular inflammation (0–2), and thus ranging 0–4. All cases with at least grade 1 steatosis were diagnosed as NAFLD independently of other criteria. When each of the three features (steatosis, ballooning, and lobular inflammation) was classified as at least grade 1, then the biopsy was categorized as NASH. For analysis of fibrosis, two groups were formed according to the severity and clinical relevance of the fibrosis, i.e., F0–1 (no or mild fibrosis) and F2–4 (moderate to advanced fibrosis).

### Transient Elastography

TE was performed prior to liver biopsy by one of two experienced specialist nurses, blinded to all other data. Examinations were performed using the FibroScan 402 system (Echosens, Paris, France), and either the M probe or the XL probe based on the computer-guided recommendation. Patients were asked to fast for at least 6 hours before the examination. TE was performed with the participant in supine position. The median value of TE-measured liver stiffness (TE-LS) in kilopascals (kPa) of at least 10 valid measurements was calculated. The examination was considered invalid if the interquartile range/median value exceeded 30%.<sup>28</sup>

### Magnetic Resonance Imaging

MRI was performed 4–8 weeks after biopsy to allow for healing. The participants were asked to fast for at least 6 hours before the examination. A 3.0-T scanner (Signa PET/MR, General Electric Healthcare, Waukesha, WI) with a 16-channel body coil was used. The 30 participants in the repeatability group underwent a second MRI within 2–4 weeks of the first scan.

### Magnetic Resonance Elastography

MRE was performed as previously described,<sup>29</sup> using a commercially available acoustic driver system (Resoundant, Rochester, MN) generating 60-Hz shear waves which were transmitted using a passive driver placed against the abdominal wall anterior to the liver. A spin-echo echo-planar imaging (SE-EPI) pulse sequence with motion-encoding gradients was used.<sup>30</sup> The acquisition parameters are listed in the Supplemental Material. Quantitative liver stiffness maps and confidence maps (elastograms) were generated on the scanner.

### MR-PDFF and R2\* Mapping

PDFF was performed using Iterative Decomposition of water and fat with Echo Asymmetry and Least squares estimation (IDEAL-IQ), a commercially available multi-echo 3D gradient-echo sequence which

has the ability to limit the confounding effects of T1 and T2\* and implements multi-peak fat model to account for the multiple resonant peaks of triglycerides.<sup>31</sup> The acquisition parameters are listed in the Supplemental Material. PDFF maps and R2\* maps (relaxation rate =  $1/T2^*$ ) were generated with IDEAL-IQ.

### T1 Mapping

Saturation Method using Adaptive Recovery Times for T1 Mapping (SMART1Map) has been described elsewhere<sup>32</sup> as a method for T1 mapping in cardiac applications. It applies a single-point saturation-recovery FIESTA technique with the ability to measure true T1. The acquisition parameters are listed in the Supplemental Material.

### Diffusion-Weighted Imaging

DWI was performed using a conventional SE-EPI sequence with *b*-values of 150 seconds/mm<sup>2</sup>, 400 seconds/mm<sup>2</sup>, and 800 seconds/mm<sup>2</sup>. The acquisition parameters are listed in the Supplemental Material. Apparent diffusion coefficient (ADC) maps were generated automatically.

### Liver Volume Measurement

A commercially available 3D gradient-echo T1-weighted sequence with two-point Dixon technique (LAVA-Flex) was used to acquire 32 axial slices through the liver in a single full-expiration breath-hold. SmartPaint software (version 1.0, Centre for Image Analysis, Uppsala University, Uppsala, Sweden) was used for post-processing the generated water-images and measuring liver volume (cm<sup>3</sup>).

### Image Analysis

An image analyst (AH) with 5 years of experience in quantitative liver MRI, blinded to histopathological and biochemical results, performed the quantitative MRI analysis using ImageJ software (version 1.50i, National Institutes of Health, Bethesda, MD). In accordance with the Quantitative Imaging Biomarker Alliance (QIBA) MRE protocol,<sup>33</sup> a free-hand region of interest (ROI) was drawn separately on each acquired slice of MRE elastograms excluding large blood vessels, the edge of the liver, fissures, and masked regions on the confidence maps. Slices with less than 500 pixels in the ROI were excluded. The ROI was cloned between the elastograms and the related anatomic/magnitude images to ensure a good anatomic correlation. The mean liver stiffness (kPa) and the ROI size (mm<sup>2</sup>) were used to calculate the overall mean MRE-measured liver stiffness (MRE-LS) in kPa, weighted by ROI size. A free-hand ROI was drawn separately on each acquired slice of the PDFF, R2\*, T1, and ADC maps using the same approach as for MRE. The mean values of all the acquired slices were obtained for PDFF (%), R2\* (second<sup>-1</sup>), and ADC (10<sup>-6</sup> mm<sup>2</sup>/second). The median value was obtained from the T1 maps (single slice) and used to calculate R1 (relaxation rate =  $1/T1$ , second<sup>-1</sup>).

A second reader (SA), a radiologist with 5 years of experience in general and abdominal radiology, blinded to histopathological and biochemical results and to the first reader's measurements, performed the analysis of MRE separately using the same approach mentioned above in order to evaluate the inter-rater reliability.

### Statistical Analysis

All statistical analyses were done using SAS software (version 9.4, SAS Institute Inc., Cary, NC) and IBM SPSS Statistics for Windows (version 27, IBM Corp., Armonk, NY). The study population was initially divided into two groups by diagnosis (NASH/NAFL). For baseline characteristics, independent samples *t*-test was used to compare continuous variables and Pearson's chi-squared test was used to compare categorical variables between the two groups. Descriptive statistics of the studied biomarkers were summarized as mean, SD, and median, and grouped according to the diagnosis (NASH/NAFL) and the dichotomized fibrosis stages (F0–1/F2–4) from the histopathology analysis. Univariate logistic regression analysis was performed

on all the biomarkers as independent variables, first with NASH/NAFL and then with F0–1/F2–4 as the dependent variable. Using logistic regression analysis, the best performing bivariate models were identified. Receiver operating characteristic curves (ROC) were used to determine the diagnostic accuracy of the univariate biomarkers and the bivariate models by calculating the area under the ROC (AUROC) and thus identifying the optimal cutoffs and the corresponding sensitivity and specificity. Spearman's correlation was used to analyze the correlation between the imaging biomarkers and the grades of activity, ballooning, lobular inflammation, and fibrosis. Repeatability of imaging biomarkers was analyzed by intra-individual coefficient of variation (CV) and intraclass correlation coefficient

**TABLE 1. Baseline Characteristics of 68 Participants With NAFLD**

Variable	Total ( <i>N</i> = 68)	NASH ( <i>N</i> = 53)	NAFL ( <i>N</i> = 15)	<i>P</i> -Value
Age (years), mean (SD)	54.5 (13.09)	53.5 (14.11)	58 (7.99)	0.122 <sup>a</sup>
Men, <i>N</i> (%)	40 (58.8%)	32 (60.4%)	8 (53.3%)	0.625 <sup>b</sup>
Women, <i>N</i> (%)	28 (41.2%)	21 (39.6%)	7 (46.7%)	
Caucasian race, <i>N</i> (%)	62 (91.2%)	47 (88.7%)	15 (100.0%)	0.172 <sup>b</sup>
BMI (kg/m <sup>2</sup> ), mean (SD)	30.8 (3.71)	31.2 (3.81)	29.1 (2.9)	0.051 <sup>a</sup>
Essential hypertension, <i>N</i> (%)	35 (51.5%)	29 (54.7%)	6 (40.0%)	0.513 <sup>b</sup>
Type 2 diabetes, <i>N</i> (%)	26 (38.2%)	24 (45.3%)	2 (13.3%)	0.037 <sup>b</sup>
Steatosis grade				
0, <i>N</i>	0	0	0	
1, <i>N</i>	22	12	10	
2, <i>N</i>	24	22	2	
3, <i>N</i>	22	19	3	
Activity grade				
0, <i>N</i>	2	0	2	
1, <i>N</i>	13	0	13	
2, <i>N</i>	44	44	0	
3, <i>N</i>	8	8	0	
4, <i>N</i>	1	1	0	
Fibrosis stage				
0, <i>N</i>	4	2	2	
1, <i>N</i>	35	25	10	
2, <i>N</i>	21	18	3	
3, <i>N</i>	5	5	0	
4, <i>N</i>	3	3	0	

NAFLD = nonalcoholic fatty liver disease; NASH = nonalcoholic steatohepatitis; NAFL = nonalcoholic fatty liver; BMI = body mass index.

<sup>a</sup>Independent samples *t*-test.

<sup>b</sup>Pearson's chi-squared test.

TABLE 2. Descriptive Statistics and Predictive Properties of Univariate TE, MRI, and Biochemical Predictors of NASH in 68 Participants With NAFLD

Variable	Summary Statistics by Group					Prediction Performance				
	Group	N	Mean	SD	Median	P-Value <sup>a</sup>	AUROC	Cutoff <sup>b</sup>	Sensitivity	Specificity
TE, kPa	NASH	51	9.45	10.8	6.9	0.009	0.77	>5.3	0.82	0.73
	NAFL	15	5.09	1.66	4.9					
MRE, kPa	NASH	49	3.13	1.57	2.7	0.028	0.74	>2.74	0.49	1.00
	NAFL	15	2.42	0.17	2.4			>2.5 <sup>c</sup>	0.65	0.80
PDFF, %	NASH	53	18.5	8.43	18	0.07	0.70	>10.4	0.81	0.60
	NAFL	15	13.7	9.29	10.2					
R2*, second <sup>-1</sup>	NASH	53	67.8	25.16	61.9	0.388	0.56	>53.4	0.79	0.40
	NAFL	15	61.8	12.76	59.4					
R1, second <sup>-1</sup>	NASH	49	1.1	0.2	1.08	0.404	0.53	>1.09	0.45	0.80
	NAFL	15	1.06	0.07	1.05					
ADC, 10 <sup>-6</sup> mm <sup>2</sup> /second	NASH	50	914	112.3	915	0.804	0.55	<830	0.24	0.93
	NAFL	15	922	106	912					
Liver volume, cm <sup>3</sup>	NASH	52	2050	541.6	1970	0.090	0.66	>1660	0.81	0.53
	NAFL	15	1780	452.3	1660					
CK18 M30, U/liter	NASH	53	257	370.7	145	0.016	0.76	>186	0.47	0.93
	NAFL	15	82.5	67.21	59					
ALT, µkat/liter	NASH	53	1.13	0.76	0.9	0.047	0.70	>0.87	0.55	0.80
	NAFL	15	0.69	0.34	0.66					
AST, µkat/liter	NASH	53	0.8	0.48	0.63	0.076	0.66	>0.63	0.55	0.80
	NAFL	15	0.58	0.15	0.56					

NAFLD = nonalcoholic fatty liver disease; NASH = nonalcoholic steatohepatitis; NAFL = nonalcoholic fatty liver; AUROC = area under the receiver operating characteristic curve; TE = transient elastography; MRE = magnetic resonance elastography; PDFF = proton density fat fraction; R2\* = relaxation rate 1/T2\*; R1 = relaxation rate 1/T1; ADC = apparent diffusion coefficient; CK18 = cytokeratin 18; ALT = alanine transaminase; AST = aspartate transaminase.

<sup>a</sup>The P-value for testing if the variable is able to predict group in univariate logistic regression analysis.

<sup>b</sup>Youden cutoff, i.e., the maximal vertical distance between the reference line and the ROC curve.

<sup>c</sup>Alternative cutoff, i.e., the minimum distance between the ROC curve and the highest point on the Y-axis.

**TABLE 3. Diagnostic Performance of Selected Bivariate Models in 68 Participants With NAFLD**

Prediction Model <sup>a</sup>		Prediction Performance				Variables in Model	
Diagnosis	Prediction Rule	AUROC	Cutoff <sup>b</sup>	Sensitivity	Specificity	Variable	P-Value <sup>c</sup>
NASH	$-12.53 + 4.6 \times \text{MRE} + 0.13 \times \text{PDFF}$	0.84	>1.38	0.74	0.87	MRE, kPa	0.008
						PDFF, %	0.009
F2–4	$-9.37 + 2.34 \times \text{MRE} + 4.16 \times \text{AST}$	0.83	>−0.08	0.68	0.92	MRE, kPa	0.017
						AST, $\mu\text{kat/liter}$	0.007
F2–4	$-8.49 + 2.6 \times \text{MRE} + 1.23 \times \text{ALT}$	0.81	>0.16	0.61	0.94	MRE, kPa	0.004
						ALT, $\mu\text{kat/liter}$	0.026

NAFLD = nonalcoholic fatty liver disease; NASH = nonalcoholic steatohepatitis; AUROC = area under the receiver operating characteristic curve; F = fibrosis stage; MRE = magnetic resonance elastography; PDFF = proton density fat fraction; ALT = alanine transaminase; AST = aspartate transaminase.

<sup>a</sup>Bivariate models constructed using logistic regression.

<sup>b</sup>The optimal cutoff (Youden cutoff), i.e., the maximal vertical distance between the reference line and the ROC curve, calculated according to the corresponding prediction rule.

<sup>c</sup>The *P*-value for the variable in the bivariate model, i.e., *P*-value for model improvement by including the variable.

(ICC). ICC was also used to analyze the inter-rater reliability between the two readers who performed MRE analysis. Statistical significance was set at  $P < 0.05$ .

## Results

### Baseline Characteristics

The study population consisted of 68 individuals with biopsy-proven NAFLD (40 men, 28 women) with a mean age of 54.5 years and a mean body mass index of  $30.8 \text{ kg/m}^2$ . NASH diagnosis was established in 53 participants and 15 were diagnosed as NAFL based on the histopathological assessment. Baseline characteristics and the distribution of different steatosis grades, activity grades, and fibrosis stages are presented in Table 1. There were no statistically significant differences between the groups, except for the frequency of type 2 diabetes which was significantly higher in the NASH group.

TE, MRE, PDFF,  $R2^*$  mapping,  $R1$  mapping, ADC, and liver volume measurement were able to be obtained in 66, 64, 68, 68, 64, 65, and 67 participants, respectively. In the second MRI examination, PDFF,  $R2^*$  mapping,  $R1$  mapping, ADC, and liver volume measurement were obtained for all the 30 participants, while MRE could be assessed in 29 participants.

The ICC of MRE analysis by two readers (inter-rater reliability) was 0.98.

### Differentiation Between NASH and NAFL

Summarized descriptive statistics for imaging and biochemical markers grouped by NASH/NAFL are presented in Table 2.

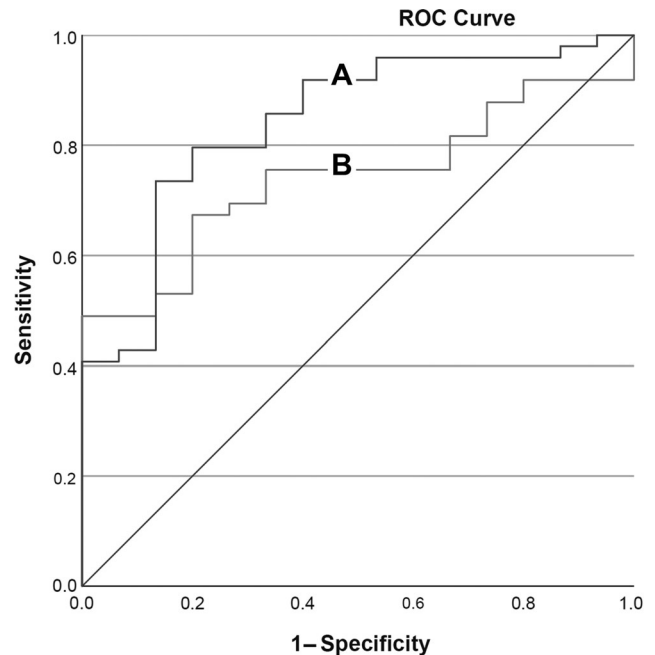


**FIGURE 1:** Receiver operating characteristic curves for diagnosing nonalcoholic steatohepatitis (NASH) displaying better performance when using a bivariate logistic regression model combining magnetic resonance elastography (MRE) with proton density fat fraction (PDFF) (area under the receiver operating characteristic curve [AUROC] 0.84,  $P = 0.008$ ) (A), than when using MRE alone (AUROC 0.74,  $P = 0.028$ ) (B).

Univariate logistic regression analysis showed significant differences between the groups in TE-LS, MRE-LS, CK18 M30, and ALT.



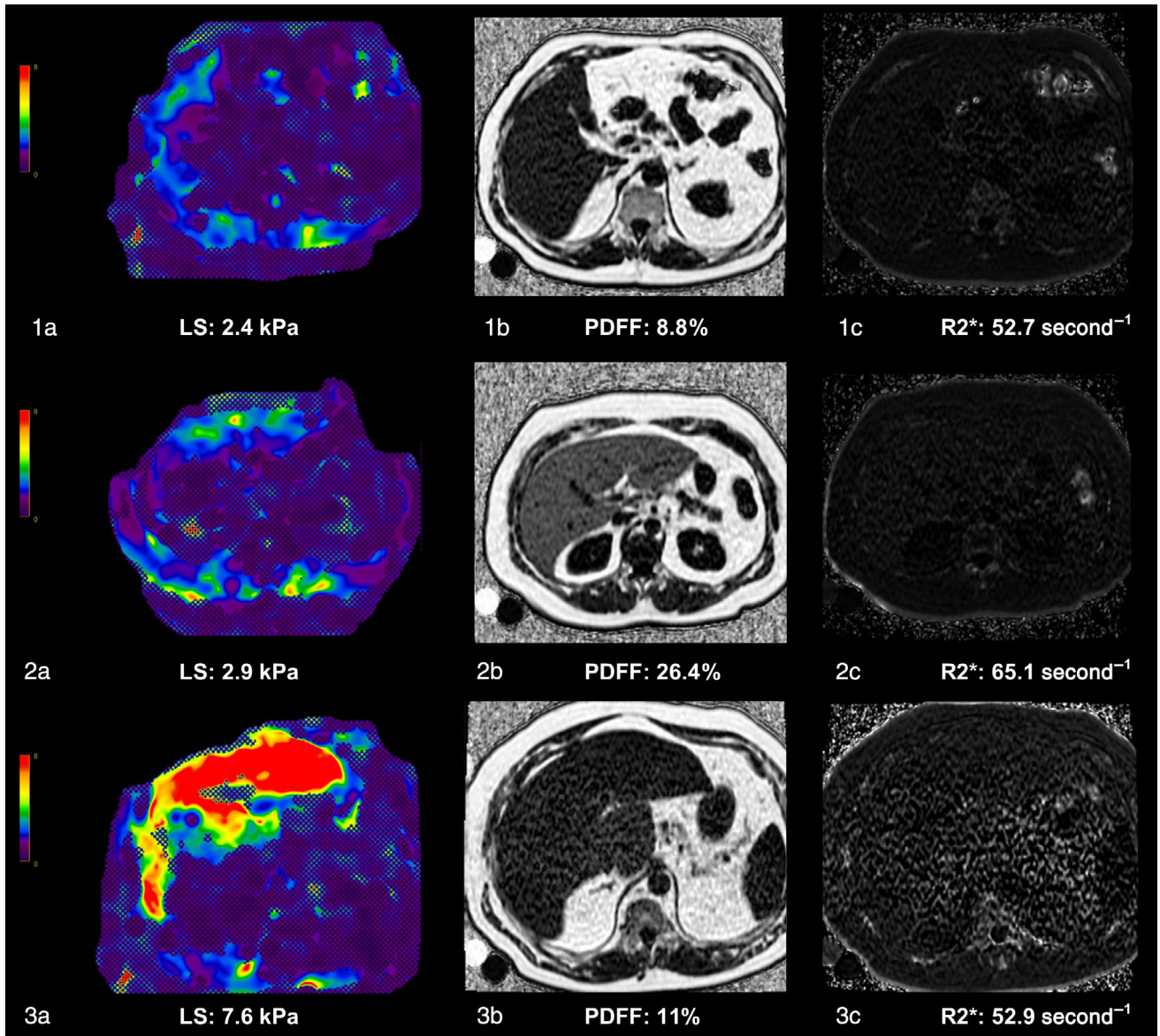


**FIGURE 2: Magnetic resonance (MR) elastograms with embedded confidence maps displaying measurement of liver stiffness (LS) (a), proton density fat fraction (PDFF) images (b), and R2\* maps (c) for three participants (1–3). The color scale in (a) is set between 0 kPa and 8 kPa. The mean LS, PDFF, and R2\* values are displayed in the figures. Liver biopsies from these three participants showed nonalcoholic fatty liver (NAFL) with fibrosis stage 1 and steatosis grade 1 (1a–1c), nonalcoholic steatohepatitis (NASH) with fibrosis stage 2 and steatosis grade 3 (2a–2c), and NASH with fibrosis stage 4 and steatosis grade 1 (3a–3c).**

In bivariate logistic regression analysis, both MRE and PDFF contributed significantly to a bivariate model for diagnosing NASH (AUROC = 0.84) (Table 3 and Fig. 1).

Combining MRE with biochemical markers did not improve the diagnostic accuracy, eg, CK18 M30, ALT, and AST showed no significant improvement of the bivariate logistic regression models combining each of them with MRE-LS ( $P = 0.51, 0.64, \text{ and } 0.158$ , respectively). Likewise, CK18 M30, ALT, and AST showed no significant improvement of the bivariate logistic regression models combining each of them with TE-LS ( $P = 0.122, 0.211, \text{ and } 0.529$ , respectively).

TE-LS, MRE-LS, and PDFF were significantly correlated with the histopathological activity grade (0–4) with Spearman's correlation coefficient of 0.41, 0.38, and 0.30, respectively (Fig. S1 in the Supplemental Material). TE-LS and MRE-LS were significantly correlated to lobular inflammation (0–2) with Spearman's correlation coefficient of 0.41 and 0.42, respectively, but not with ballooning ( $P = 0.075$  and 0.303, respectively). PDFF was significantly correlated with ballooning (0–2) with Spearman's correlation coefficient of 0.25, but not with lobular inflammation ( $P = 0.109$ ) (Fig. S2 in the Supplemental Material).

MR elastograms, PDFF, R2\*, T1, and ADC maps for three participants with different histopathological findings,

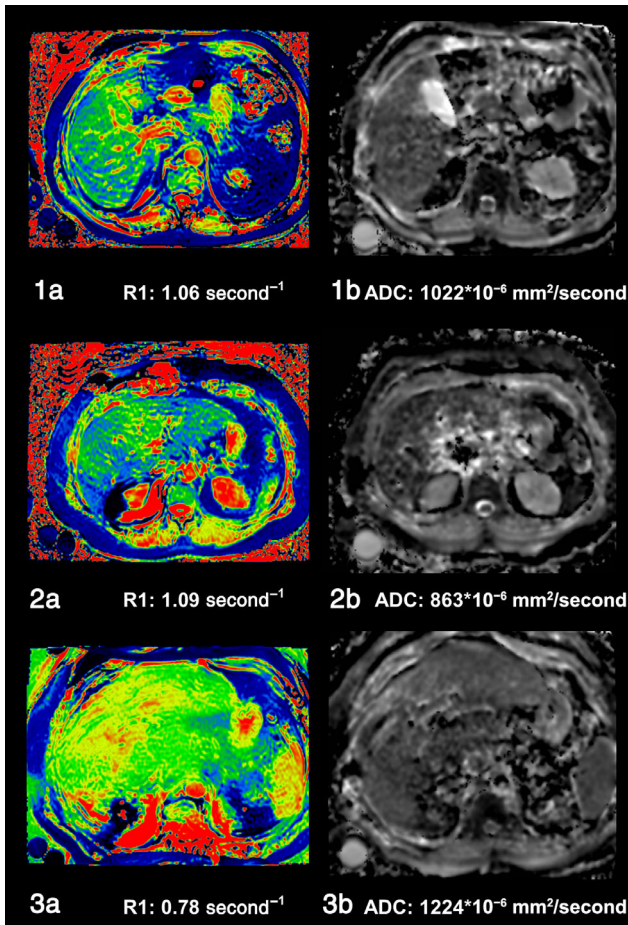


**FIGURE 3:** T1 maps (a) and apparent diffusion coefficient (ADC) maps (b) for the same three participants as in Figure 2 (1–3). The R1 and ADC values are displayed in the figures. Liver biopsies from these three participants showed nonalcoholic fatty liver (NAFL) with fibrosis stage 1 and steatosis grade 1 (1a–1b), nonalcoholic steatohepatitis (NASH) with fibrosis stage 2 and steatosis grade 3 (2a–2b), and NASH with fibrosis stage 4 and steatosis grade 1 (3a–3b).

i.e., both NAFL and NASH and with different stages of fibrosis and steatosis, are shown in Figs. 2 and 3.

### Differentiation Between F0–1 and F2–4

Summarized descriptive statistics for imaging and biochemical markers grouped by F0–1 and F2–4 are presented in Table 4. Univariate logistic regression analysis showed significant differences between these groups with TE-LS, MRE-LS, ALT, and AST (AUROC = 0.89, 0.74, 0.72, and 0.77, respectively).

In bivariate logistic regression analysis, two models combining MRE-LS with AST (AUROC = 0.83), and MRE-LS with ALT (AUROC = 0.81) showed a significantly better performance in diagnosing F2–4, compared with MRE-LS, ALT, or AST alone (Table 3). TE-LS, MRE-LS, R1, and liver volume were significantly correlated with the histopathological fibrosis stage (0–4) with Spearman's correlation coefficient of 0.71, 0.49, −0.3, and 0.26, respectively.

### Repeatability of Imaging Biomarkers

The mean interval between the first and second MRI was 23.5 (range 14–48) days. The CV and ICC values of the imaging biomarkers are listed in Table 5. The ICC of MRE, PDFF, R2\*, and liver volume was higher than 0.9. MR images demonstrating the repeatability in two different participants are displayed in Figs. S3 and S4 in the Supplemental Material.

### Discussion

In our study, liver stiffness measured by both TE and MRE could differentiate NASH from NAFL. Prior prospective studies which tested the ability of MRE to differentiate between NASH and NAFL have reported cutoff values between 2.53 and 3.26 (AUROC 0.70–0.79).<sup>24,34,35</sup> In the present study, a cutoff value of 2.74 kPa (2.5 kPa if the minimum distance between the ROC curve and the highest point on the Y-axis was used) could be identified with an AUROC of 0.74. The fact that cutoff values vary between studies might be explained by demographic differences, differences in study designs and in the used technique to obtain and analyze MRE. Furthermore, the diagnosis of NASH is complicated by the heterogeneity of the histopathological findings, the variations in biopsy sampling and interpretation, and the variations in the available histopathological scoring systems.<sup>6,16,17</sup> A major difference between our study and the above-mentioned studies<sup>24,34,35</sup> is the histopathological scoring system used. Those studies used the NASH Clinical Research Network scoring system,<sup>36</sup> while the present study used the newer SAF scoring system,<sup>5</sup> which offers a more distinct definition of NASH. Technically, obtaining seven slices for MRE through the liver in full-inspiration instead of the routinely used technique of four slices in full-expiration might cause differences when comparing the MRE results of the present study with previous studies. Full-inspiration was preferred since abdominal obesity is common in NAFLD. Thus, in full-expiration, the liver might be positioned too cranially to permit adequate transfer of the acoustic waves into the liver.

A bivariate logistic regression model combining MRE-LS with PDFF showed a better performance in diagnosing NASH than MRE-LS alone. This might be partly explained by the observation that MRE-LS was correlated to lobular inflammation and PDFF was correlated to ballooning, which are the two components used for NASH diagnosis in the SAF scoring system. A similar model combining gradient-echo MRE and PDFF showed an AUROC of 0.87 in a recently published study.<sup>37</sup> In another study,<sup>38</sup> a multiparametric MR index, combining MRE, PDFF (determined by magnetic resonance spectroscopy), and T1 mapping, could diagnose NASH with AUROC of 0.883. In the present study, R1, calculated from T1 mapping, could not diagnose NASH or F2–4. However, there is yet no reference standard method for liver T1 mapping and the method used in our study (SMART1Map applying a single-point saturation-recovery technique) differs from the method used in the other study (Look-



**TABLE 4. Descriptive Statistics and Predictive Properties of Univariate TE, MRI and Biochemical Predictors of Fibrosis Stages 0–1 and 2–4 in 68 Participants With NAFLD**

Variable	Summary Statistics by Group					Prediction Performance				
	Group	N	Mean	SD	Median	P-Value <sup>a</sup>	AUROC	Cutoff <sup>b</sup>	Sensitivity	Specificity
TE, kPa	F0-1	39	5.45	1.72	5.4	<0.0001	0.89	>6.4	0.89	0.77
	F2-4	27	12.8	14.04	9.1					
MRE, kPa	F0-1	36	2.5	0.26	2.46	0.004	0.74	>2.82	0.54	0.92
	F2-4	28	3.56	1.97	2.86					
PDFF, %	F0-1	39	17.1	9.71	15.3	0.746	0.56	>10.4	0.86	0.38
	F2-4	29	17.8	7.5	17.8					
R2*, second <sup>-1</sup>	F0-1	39	69.1	27.89	62.2	0.297	0.54	<59.3	0.55	0.62
	F2-4	29	62.9	13.91	57.4					
R1, second <sup>-1</sup>	F0-1	38	1.12	0.18	1.08	0.078	0.67	<1	0.50	0.89
	F2-4	26	1.04	0.17	1					
ADC, 10 <sup>-6</sup> mm <sup>2</sup> /second	F0-1	36	907	114.3	911	0.48	0.55	>924	0.59	0.61
	F2-4	29	927	105.8	929					
Liver volume, cm <sup>3</sup>	F0-1	38	1890	481.4	1820	0.085	0.63	>1730	0.86	0.45
	F2-4	29	2120	573.6	2000					
CK18 M30, U/liter	F0-1	39	146	265.8	88	0.1	0.76	>139	0.72	0.74
	F2-4	29	315	396.5	214					
ALT, µkat/liter	F0-1	39	0.82	0.49	0.67	0.012	0.72	>0.78	0.79	0.69
	F2-4	29	1.32	0.87	1.03					
AST, µkat/liter	F0-1	39	0.58	0.16	0.55	0.001	0.77	>0.66	0.72	0.79
	F2-4	29	0.98	0.58	0.82					

NAFLD = nonalcoholic fatty liver disease; F = fibrosis stage; AUROC = area under the receiver operating characteristic curve; TE = transient elastography; MRE = magnetic resonance elastography; PDFF = proton density fat fraction; R2\* = relaxation rate 1/T2\*; R1 = relaxation rate 1/T1; ADC = apparent diffusion coefficient; CK18 = cytokeratin 18; ALT = alanine transaminase; AST = aspartate transaminase.

<sup>a</sup>The P-value for testing if the variable is able to predict group in univariate logistic regression analysis.

<sup>b</sup>Youden cutoff, i.e., the maximal vertical distance between the reference line and the ROC curve.

**TABLE 5. Repeatability Analysis of Imaging Parameters**

Variable	N	CV	ICC
MRE, kPa	29	0.09	0.94
PDFF, %	30	0.04	0.99
R2*, second <sup>-1</sup>	30	0.04	0.96
R1, second <sup>-1</sup>	30	0.10	0.47
ADC, 10 <sup>-6</sup> mm <sup>2</sup> /second	30	0.07	0.76
Liver volume, cm <sup>3</sup>	30	0.04	0.98

CV = intra-individual coefficient of variation; ICC = intraclass correlation coefficient; MRE = magnetic resonance elastography; PDFF = proton density fat fraction; R2\* = relaxation rate 1/T2\*; R1 = relaxation rate 1/T1; ADC = apparent diffusion coefficient.

Locker inversion recovery technique). Likewise, the used DWI sequence might not be optimal for diagnosing NASH.

In addition to its known role in accurately quantifying steatosis,<sup>39</sup> PDFF showed a potential role in improving the performance of MRE in diagnosing NASH in the present study. Even though the PDFF cutoff value for NASH of 10.4% was not statistically significant in the present study, it differs from the reported cutoff between normal and steatotic liver parenchyma of 5.2%.<sup>23</sup> Moreover, the MRE cutoff for NASH (2.5 kPa or 2.74 kPa), which was statistically significant in the present cohort of individuals with confirmed NAFLD, did not differ substantially from the cutoff reported in another study in individuals with or without NAFLD (2.49).<sup>35</sup> This suggests that MRE and PDFF might be needed to be assessed in combination to diagnose NASH.

TE and MRE could differentiate between F2–4 (moderate to advanced fibrosis) and F0–1 (no or mild fibrosis). In a recently published meta-analysis<sup>40</sup> including 12 studies, MRE was found to have a pooled AUROC of 0.93 and cutoff values ranging from 2.38 kPa to 5.37 kPa to diagnose F2–4. In the present study, the cutoff was 2.82. Another meta-analysis<sup>22</sup> concluded that MRE has a higher diagnostic accuracy in grading fibrosis than TE, with an AUROC of 0.92 and 0.87 for MRE and TE, respectively, for diagnosing F2–4. A recent prospective study<sup>25</sup> stated the same conclusion with an AUROC of 0.85 and 0.75, while another recent prospective study<sup>26</sup> showed an AUROC of 0.85 and 0.77, but with no statistically significant difference between the AUROC values for MRE and TE, respectively, for diagnosing F2–4. In the present study, TE had a higher AUROC than MRE for diagnosing F2–4. This might be influenced by the fact that TE acquired data from the same liver lobe where biopsy was performed. Furthermore, TE was performed on the same day as liver biopsy in most participants (those with no recent biopsy available), while MRI was performed 4–8 weeks after biopsy.

Two bivariate logistic regression models combining MRE with AST and MRE with ALT showed better performance in diagnosing F2–4 than the single univariate biomarkers and improved the AUROC. However, the diagnostic performance of ALT as well as CK18 M30, as univariate biomarkers or in the model combining MRE with ALT for diagnosing F2–4, has to be interpreted cautiously, as both were considered as optional inclusion criteria.

It is important to point out that the results presented in this study, including different cut-off values and bivariate models to differentiate between NASH and NAFL and between F2–4 and F0–1, were determined in a cohort of adult participants with biopsy-proven NAFLD. Thus, these results are considered applicable only when there is clinical suspicion of NAFLD and the presence of hepatic steatosis without any secondary cause of hepatic fat accumulation has been confirmed. MRI-based techniques, primarily PDFF, can readily confirm and grade hepatic steatosis<sup>20</sup> which is the first hallmark in the diagnosis of NAFLD.

A strength of the present study was the wide range of imaging biomarkers that were compared in the same population. Another strength was the excellent repeatability of most of the studied imaging biomarkers, including MRE and PDFF, as well as the high inter-rater reliability of MRE. The results of this study emphasize the potential role of quantitative MRI techniques in diagnosing and grading diffuse liver diseases when included as a part of a multiparametric MRI liver protocol in clinical practice, and thus reducing the need for liver biopsy.

### Limitations

A limitation of the present study was the small number of participants, particularly participants having advanced fibrosis (F3–4) ( $N = 8$ ), limiting the possibility to study the differentiation between the individual fibrosis stages. The skewed populations of NASH vs. NAFL were another limitation.

### Conclusions

Our study demonstrated that liver stiffness measurement by both TE and MRE could identify individuals with NASH and differentiate between those with no or mild fibrosis and those with moderate and higher stages of fibrosis. Combining MRE with PDFF improved the diagnosis of NASH, implying that specific imaging parameters might reflect specific histological criteria.

### Acknowledgments

The main funding body of The Swedish CARDioPulmonary bioImage Study (SCAPIS) is the Swedish Heart-Lung Foundation. The study is also funded by the Knut and Alice Wallenberg Foundation, the Swedish Research Council and VINNOVA (Sweden's Innovation Agency), the University of Gothenburg and Sahlgrenska University Hospital, Karolinska Institutet and Stockholm County Council, Linköping

University and University Hospital, Lund University and Skåne University Hospital, Umeå University and University Hospital, Uppsala University and University Hospital.

## Conflict of Interest

Heiko G. Niessen, Corinna Schoelch, and Christian Schultheis are employees of Boehringer Ingelheim Pharma GmbH & Co. KG.

## REFERENCES

1. Younossi ZM, Koenig AB, Abdelatif D, Fazel Y, Henry L, Wymer M. Global epidemiology of nonalcoholic fatty liver disease—Meta-analytic assessment of prevalence, incidence, and outcomes. *Hepatology* 2016; 64(1):73-84.
2. Chalasani N, Younossi Z, Lavine JE, et al. The diagnosis and management of nonalcoholic fatty liver disease: Practice guidance from the American Association for the Study of Liver Diseases. *Hepatology* 2018;67(1):328-357.
3. Godoy-Matos AF, Silva Junior WS, Valerio CM. NAFLD as a continuum: From obesity to metabolic syndrome and diabetes. *Diabetol Metab Syndr* 2020;12:60.
4. Stahl EP, Dhindsa DS, Lee SK, Sandesara PB, Chalasani NP, Sperling LS. Nonalcoholic fatty liver disease and the heart: JACC state-of-the-art review. *J Am Coll Cardiol* 2019;73(8):948-963.
5. Bedossa P, Poitou C, Veyrie N, et al. Histopathological algorithm and scoring system for evaluation of liver lesions in morbidly obese patients. *Hepatology* 2012;56(5):1751-1759.
6. Brown GT, Kleiner DE. Histopathology of nonalcoholic fatty liver disease and nonalcoholic steatohepatitis. *Metabolism* 2016;65(8):1080-1086.
7. Singh S, Allen AM, Wang Z, Prokop LJ, Murad MH, Loomba R. Fibrosis progression in nonalcoholic fatty liver vs nonalcoholic steatohepatitis: A systematic review and meta-analysis of paired-biopsy studies. *Clin Gastroenterol Hepatol* 2015;13(4):643-654, e641-649; quiz e639-640.
8. Nasr P, Ignatova S, Kechagias S, Ekstedt M. Natural history of non-alcoholic fatty liver disease: A prospective follow-up study with serial biopsies. *Hepatol Commun* 2018;2(2):199-210.
9. Kleiner DE, Brunt EM, Wilson LA, et al. Association of histologic disease activity with progression of nonalcoholic fatty liver disease. *JAMA Netw Open* 2019;2(10):e1912565.
10. Schwabe RF, Tabas I, Pajvani UB. Mechanisms of fibrosis development in nonalcoholic steatohepatitis. *Gastroenterology* 2020;158(7):1913-1928.
11. Cholaneril G, Patel R, Khurana S, Satapathy SK. Hepatocellular carcinoma in non-alcoholic steatohepatitis: Current knowledge and implications for management. *World J Hepatol* 2017;9(11):533-543.
12. Stine JG, Wentworth BJ, Zimmet A, et al. Systematic review with meta-analysis: Risk of hepatocellular carcinoma in non-alcoholic steatohepatitis without cirrhosis compared to other liver diseases. *Aliment Pharmacol Ther* 2018;48(7):696-703.
13. Haldar D, Kern B, Hodson J, et al. Outcomes of liver transplantation for non-alcoholic steatohepatitis: A European Liver Transplant Registry study. *J Hepatol* 2019;71(2):313-322.
14. Dulai PS, Singh S, Patel J, et al. Increased risk of mortality by fibrosis stage in nonalcoholic fatty liver disease: Systematic review and meta-analysis. *Hepatology* 2017;65(5):1557-1565.
15. Taylor RS, Taylor RJ, Bayliss S, et al. Association between fibrosis stage and outcomes of patients with nonalcoholic fatty liver disease: A systematic review and meta-analysis. *Gastroenterology* 2020;158(6):1611-1625.e12.
16. Ratzliff V, Charlotte F, Heurtier A, et al. Sampling variability of liver biopsy in nonalcoholic fatty liver disease. *Gastroenterology* 2005; 128(7):1898-1906.
17. Sumida Y, Nakajima A, Itoh Y. Limitations of liver biopsy and non-invasive diagnostic tests for the diagnosis of nonalcoholic fatty liver disease/nonalcoholic steatohepatitis. *World J Gastroenterol* 2014;20(2): 475-485.
18. Castera L, Friedrich-Rust M, Loomba R. Noninvasive assessment of liver disease in patients with nonalcoholic fatty liver disease. *Gastroenterology* 2019;156(5):1264-1281.e4.
19. Zhou JH, Cai JJ, She ZG, Li HL. Noninvasive evaluation of nonalcoholic fatty liver disease: Current evidence and practice. *World J Gastroenterol* 2019;25(11):1307-1326.
20. Qu Y, Li M, Hamilton G, Zhang YN, Song B. Diagnostic accuracy of hepatic proton density fat fraction measured by magnetic resonance imaging for the evaluation of liver steatosis with histology as reference standard: A meta-analysis. *Eur Radiol* 2019;29(10):5180-5189.
21. Singh S, Venkatesh SK, Loomba R, et al. Magnetic resonance elastography for staging liver fibrosis in non-alcoholic fatty liver disease: A diagnostic accuracy systematic review and individual participant data pooled analysis. *Eur Radiol* 2016;26(5):1431-1440.
22. Hsu C, Caussy C, Imajo K, et al. Magnetic resonance vs transient elastography analysis of patients with nonalcoholic fatty liver disease: A systematic review and pooled analysis of individual participants. *Clin Gastroenterol Hepatol* 2019;17(4):630-637.e8.
23. Imajo K, Kessoku T, Honda Y, et al. Magnetic resonance imaging more accurately classifies steatosis and fibrosis in patients with nonalcoholic fatty liver disease than transient elastography. *Gastroenterology* 2016; 150(3):626-637.e7.
24. Park CC, Nguyen P, Hernandez C, et al. Magnetic resonance elastography vs transient elastography in detection of fibrosis and non-invasive measurement of steatosis in patients with biopsy-proven non-alcoholic fatty liver disease. *Gastroenterology* 2017;152(3):598-607.e2.
25. Lefebvre T, Wartelle-Bladou C, Wong P, et al. Prospective comparison of transient, point shear wave, and magnetic resonance elastography for staging liver fibrosis. *Eur Radiol* 2019;29(12):6477-6488.
26. Furlan A, Tublin ME, Yu L, Chopra KB, Lippello A, Behari J. Comparison of 2D shear wave elastography, transient elastography, and MR elastography for the diagnosis of fibrosis in patients with nonalcoholic fatty liver disease. *AJR Am J Roentgenol* 2020;214(1):W20-W26.
27. Bergstrom G, Berglund G, Blomberg A, et al. The Swedish CARDioPulmonary BioImage Study: Objectives and design. *J Intern Med* 2015; 278(6):645-659.
28. Castera L, Forns X, Alberti A. Non-invasive evaluation of liver fibrosis using transient elastography. *J Hepatol* 2008;48(5):835-847.
29. Venkatesh SK, Yin M, Ehman RL. Magnetic resonance elastography of liver: Technique, analysis, and clinical applications. *J Magn Reson Imaging* 2013;37(3):544-555.
30. Mariappan YK, Dzyubak B, Glaser KJ, et al. Application of modified spin-echo-based sequences for hepatic MR elastography: Evaluation, comparison with the conventional gradient-echo sequence, and preliminary clinical experience. *Radiology* 2017;282(2):390-398.
31. Reeder SB, Robson PM, Yu H, et al. Quantification of hepatic steatosis with MRI: The effects of accurate fat spectral modeling. *J Magn Reson Imaging* 2009;29(6):1332-1339.
32. Matsumoto S, Okuda S, Yamada Y, et al. Myocardial T1 values in healthy volunteers measured with saturation method using adaptive recovery times for T1 mapping (SMART1Map) at 1.5 T and 3 T. *Heart Vessels* 2019;34(11):1889-1894.
33. QIBA MR Biomarker Committee. MR Elastography of the Liver, Quantitative Imaging Biomarkers Alliance. Profile Stage: Consensus. May 2, 2018. Available from: <http://qibawiki.rsna.org/index.php/Profiles>
34. Loomba R, Wolfson T, Ang B, et al. Magnetic resonance elastography predicts advanced fibrosis in patients with nonalcoholic fatty liver disease: A prospective study. *Hepatology* 2014;60(6):1920-1928.

35. Costa-Silva L, Ferolla SM, Lima AS, Vidigal PVT, Ferrari TCA. MR elastography is effective for the non-invasive evaluation of fibrosis and necroinflammatory activity in patients with nonalcoholic fatty liver disease. *Eur J Radiol* 2018;98:82-89.
36. Kleiner DE, Brunt EM, Van Natta M, et al. Design and validation of a histological scoring system for nonalcoholic fatty liver disease. *Hepatology* 2005;41(6):1313-1321.
37. Dzyubak B, Li J, Chen J, et al. Automated analysis of multiparametric magnetic resonance imaging/magnetic resonance elastography exams for prediction of nonalcoholic steatohepatitis. *J Magn Reson Imaging* 2021;54(1):122-131.
38. Kim JW, Lee YS, Park YS, et al. Multiparametric MR index for the diagnosis of non-alcoholic steatohepatitis in patients with non-alcoholic fatty liver disease. *Sci Rep* 2020;10(1):2671.
39. Idilman IS, Keskin O, Celik A, et al. A comparison of liver fat content as determined by magnetic resonance imaging-proton density fat fraction and MRS versus liver histology in non-alcoholic fatty liver disease. *Acta Radiol* 2016;57(3):271-278.
40. Liang Y, Li D. Magnetic resonance elastography in staging liver fibrosis in non-alcoholic fatty liver disease: A pooled analysis of the diagnostic accuracy. *BMC Gastroenterol* 2020; 20(1):89.